Jurnal
Teknologi

Full Paper

A MORPHOLOGICAL STUDY OF NICKEL OXIDE HOLLOW FIBER MEMBRANES: EFFECT OF AIR GAP & SINTERING TEMPERATURE

Mohd Izzat Iqbal Mohd Zahar, Mohd Hafiz Dzarfan Othman*, Mukhlis A Rahman, Juhana Jaafar, Siti Khadijah Hubadillah

Advanced Membrane Technology Research Centre (AMTEC), Faculty of Chemical and Energy Engineering, University Teknologi Malaysia, 81310 UTM Johor Bahru, Johor, Malaysia

Article history
Received
24 August 2016
Received in revised form
10 October 2016
Accepted
3 November 2016

*Corresponding author
dzarfan@utm.my

Graphical abstract

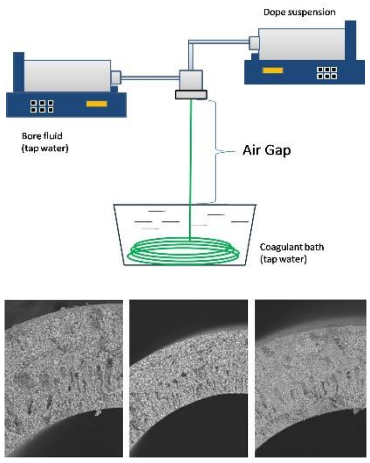

Abstract

A systematic study of the air gap effects on morphology and mechanical strength of Nickel Oxide (NiO) hollow fiber membranes has been carried out. The hollow fibers were prepared using the dry-jet wet spinning process using a dope solution containing NiO/N-methyl-2-pyrrolidone (NMP)/Arlacel/Poly(ethylene sulphide) with a weight ratio of 70/22.9/0.1/7. Tap water was used as internal and external coagulants. The cross-sectional structure of precursors hollow fiber membrane was studied by scanning electron microscopy (SEM). The results showed that both inner and outer finger-like voids of the hollow membrane were determined by the air gap distance. Experimental results indicated that an increase in air gap distance, from 100 mm to 200 mm, gave a hollow fiber with a lower mechanical strength and higher percentages of cross section surface area covered by finger-like voids structures. This study also revealed that the air gap introduced an elongation stress because of gravity on the internal or external surfaces of the NiO hollow fibers. A more effective hollow fiber membrane which is in asymmetric structure instead of symmetric structure can be produced by using air gap higher than 200 mm.

Keywords: Nickel Oxide, asymmetric hollow fiber membrane, air gap, sintering temperature

Abstrak

Satu kajian sistematik terhadap kesan jurang udara terhadap morfologi dan kekuatan mekanikal bagi nikel oksida (NiO) membran gentian berongga. Ianya telah disediakan dengan menggunakan kaedah 'dry-jet wet spinning process' yang mengandungi NiO/N-methyl-2-pyrrolidone (NMP)/Arlacel/Poly(ethylene sulphide) dengan nisbah berat 70/22.9/0.1/7. Air paip telah digunakan sebagai koagulan dalaman dan luaran. Struktur keratan rentas prekursor membran telah dikaji menggunakan mesin pegimbas mikroskop elektron (SEM). Hasil kajian menunjukkan bahawa panjang gentian membran berongga yang terbentuk dari permukaan dalam dan luar adalah ditentukan oleh jarak ruang udara. Keputusan eksperimen menunjukkan bahawa peningkatan dalam jarak jurang udara, dari 100 mm hingga 200 cm, membentuk membran dengan kekuatan mekanikal yang lebih rendah dan peratusan 'finger-like voids' yang lebih tinggi. Kajian ini juga menunjukkan bahawa jurang udara menyebabkan tekanan pemanjangan terhadap membran oleh tarikan gravity bumi. Pada ketinggian ruang udara 200 mm, struktur simetrik serat berongga boleh diubah kepada struktur asimetrik dimana ianya lebih berkesan dalam penggunaan membran.

Kata kunci: Nikel oksida, asimetrik membrane, jurang udara, suhu sinter

1.0 INTRODUCTION

Conventional membranes can be made of polymers or inorganic materials which are ceramic, carbon or metal. In recent technology, the most recognizable water treatment membranes are made from polymer. By preparing asymmetric metal membrane, i.e. nickel hollow fiber, this study will provide alternative to conventional organic membrane. By focusing in inorganic membrane it is a move towards producing high quality traits such as negligible permeability to the liquid and nonvolatile components, high porosity for the vapor phase, high defiance to heat flow by conduction, an economically most favorable membrane thickness, low moisture adsorptivity and a commercially long life span with saline solutions under the operating condition [1]. Nickel Oxide (NiO) has been identified as suitable ceramic as it could withstand high operating temperature of more than 1000°C and much superior mechanical strength [2-4]. Compared to polymeric or other ceramic membranes, it is stable under aggressive solvents, good chemical resistance, has low fouling rate and high flux making it cost effective in the long run.

In general, the membrane structure can be divided into asymmetric and symmetric membrane as shown in Figure 1. As a rule of thumb, the permeate flux through a membrane is inversely proportional to the membrane thickness. A high permeability is desirable in membrane separation process for economic reasons. Therefore, the selective layer of membrane thickness should be as thin and dense as possible.

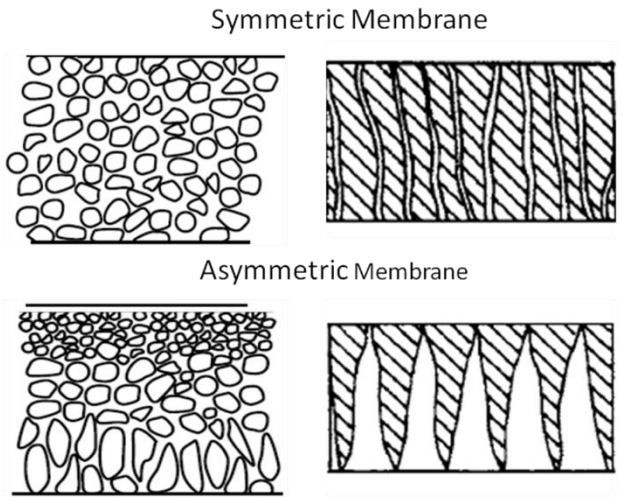

Figure 1 Morphology of symmetric and asymmetric membrane (A) shows sponge-like voids formation while (B) shows finger-like voids formation

Conventional film fabrication technology limits the production of mechanically strong, defect-free films to minimum of 20μm thickness [5]. Subsequently, the development of asymmetric membrane fabrication technique was seen as one of the major breakthroughs of membrane fabrication technology. Asymmetric structure has been identified as optimum structure for membrane. An asymmetric ceramic membrane usually consists of an extremely thin and dense top layer with separation properties, over a thicker porous support [6]. As the rejection properties and flow rates of the membrane are determined entirely by the surface layer, the support layer functions as a mechanical support which give advantages of higher fluxes and selectivity.

Loeb and Sourirajan first describe production of asymmetric polymeric membrane formation which is known as phase inversion technique [7]. After the addition of certain amount of ceramic powder to polymeric solution (polymer and solvent) it will be well mixed to produce suspension solution. Afterwards this suspension solution will be immersed in a non-solvent which is miscible with the solvent. Then solvent/non-solvent exchange will take place leading to precipitation of the polymer phase. Ceramic particles are immobilized once precipitation has taken place and the membrane macro structure can be largely established at this point by manipulating and adjusting the various parameters of the phase inversion process. Immense effort has been made to control and understands the formation mechanisms for the wide range of structures observed in polymeric membrane formation [8-11]. Nonetheless there are huge differences between polymeric and ceramic membrane, since only low concentration of polymer is used during ceramic membrane preparation. To date, only two morphologies can be observed in both ceramic and polymer membrane which are finger-like voids and a sponge-like structure. In general, the macrostructure such as finger-like structure of the fiber precursor designed during the phase inversion process is retained after sintering process. However, at high sintering temperature, sponge-like regions will become denser and eventually become gas tight for some ceramic materials [12].

The formation of finger-like voids in ceramic membrane precursors can be explained by hydrodynamically unstable viscous fingering that occurs at the interface between fluids with different viscosities in the first moment of mixing. A steep concentration gradient between suspension and non-solvent results in solvent and non-solvent exchange which will increase viscosity of suspension and eventually results in precipitation of the polymer phase. On the other hand, viscous fingering occurs due to instabilities at the interface between the suspension and the coagulant, initiating the formation of finger-like voids [7]. The relative thickness of finger-like and sponge-like regions greatly affects the properties of the membrane such as membrane mechanical strength and permeation flux. Due to the versatility of ceramic hollow fiber membranes, it is

essential that fiber morphology can be controlled so that it may be tailored to a specific application.

The sintering process is the final stage in the preparation of ceramic membranes. This process removes organic material such as water and polymer and leaves membrane with pure ceramic materials. Various studies reported that this process affect the morphology of the ceramic membrane. Experimental data has shown that increase in sintering temperature would enhance the mechanical strength. Lie *et al.* has conducted an experiment on Alumina (Al_2O_3) and after 10 hours of sintering it shows that higher temperature sintering will results higher mechanical strength [13]. Besides that, Liu and Li [14] who prepared SCYb hollow fiber membranes reported that the surface of the ceramic membranes changed with an increase in the sintering temperature from 600 °C to 1600 °C where the ceramic particles started to form larger grain size as the temperature increases and became completely dense at 1600 °C. Tan *et al.* [15] indicated that the surface morphology such as pore size and diameter of alumina hollow fiber changed as sintering temperature increased.

This study shows that by using NiO as its ceramic content while controlling the air gap length, the finger-like voids can be initiated from both the inner and outer surfaces simultaneously or from the inner surface alone. Outer surface finger-like void length varies between 10% of the fiber thickness, i.e. asymmetric membrane structure, to completely diminished, i.e. symmetric membrane. The present work is, therefore, to examine how the choice of air gap distance affects the ceramic membrane morphology.

2.0 METHODOLOGY

Asymmetric NiO hollow fiber membrane was prepared by using dry-jet wet extrusion technique. The ceramic suspension was prepared by mixing NiO with N-methyl-2-pyrrolidone (NMP), Arlacel, and Poly(ethylene sulphide) (PESf) that act as solvent, dispersant and polymer binder respectively. Details of suspension loading are shown in Table 1. The 0.1 wt. % of Arlacel was first dissolved in the NMP solution. NiO powder was added gradually while stirring in Alumina pot.

Afterwards, ceramic suspension was rolled with one 22.0 mm and eight 10.5 mm alumina ceramic balls in planetary ball mill (Magna NQM-2L Planetary Ball Mill). Rate of planetary ball mill was constantly set at 203 rpm for 48 hours. The milling was maintained for further 48 hours after the addition of polymer binder, with NiO:PESf ratio of 10:1. The planetary ball mill was used to ensure that all the powders were dispersed uniformly in the polymer solution. The alumina ceramic milling balls were removed and the suspension was degassed for 1 hour with lowest RPM of spinner (79 - 91 RPM) to ensure that there are no microscopic air bubbles entrapped inside the ceramic suspension. Afterwards viscosity test was conducted using Brookfield Digital Viscometer (DV-I Prime). Spinning process was carried out using parameters shown in Table 2. Tap water was used as the internal and external coagulants. Schematic diagram of the spinning process experimental setup is shown in Figure 2. The formed hollow fiber NiO precursors were immersed in water bath for 24 hours to complete the phase inversion process. The precursor fibers were straighten and dried under room temperature. Afterwards, precursors are sintered at target temperature (T_C) of 1200 °C, 1300 °C, 1400 °C and 1500 °C following sintering profile as shown in Figure 3.

Table 1 Ceramic suspension loading of NiO hollow fiber

Fiber	Composition (wt. %)
NiO	70
PESf	7
Alracel	0.1
NMP	22,9

Table 2 Spinning parameters of NiO hollow fiber

Spinning parameter	M1	M2	M3
Outer spinneret diameter (mm)		1.20	
Inner spinneret diameter (mm)		2.80	
Air gap (mm)	100	150	200
Extrusion rate (ml/min)		8	
Bore fluid rate (ml/min)		10	

3.0 RESULTS AND DISCUSSION

Viscosity of spinning suspension has been identified as benchmark and integral factors to determine the morphology of precursor membranes. Figure 4 shows the viscosity at shear rate ranging from 5 s^{-1} to 100 s^{-1} for Nickel Oxide suspension prior to spinning process. The trend line of the viscosity against shear rate shows non-Newtonian behaviour that was similar to the general ceramic material and was found to be shear thinning. At sheer rate of 30 s^{-1}, the viscosity calculated is 7,120 cP. This viscosity value, which is below 22,000 cP indicates that possibility of finger-like micro voids formation during phase inversion of ceramic suspension. According to Kingsbury & Li [7], critical viscosity values higher than this threshold value will hamper the formation of finger-like voids and producing isolated voids also known as sponge-like structure instead.

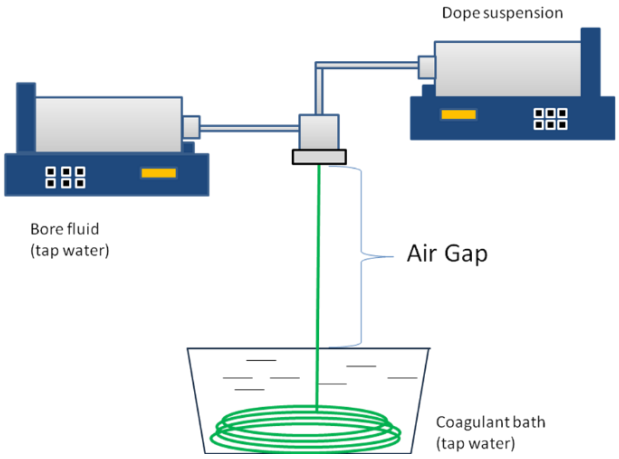

Figure 2 Schematic diagram of experimental setup during spinning process

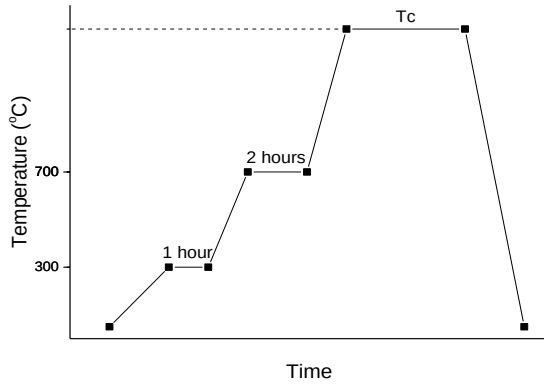

Figure 3 Sintering profile with with target temperature (T_c) of (1200 °C, 1300 °C, 1400 °C and 1500 °C)

Figure 5 shows hollow fibers spun at air gap of (A) 100 mm, (B) 150 mm and (C) 200 mm respectively. At air gap of 100 mm, the precursor shows sandwich finger-like voids. As air gap is increased, the outer length of finger-like voids decrease and eventually at the air gap of 200 mm this outer finger-like structure completely diminished. The morphology of fiber shown in Figure 5 is believed to be the results of hydrodynamically unstable viscous fingering that occurs concurrently and to similar extent at both the inner and outer fiber surfaces. However, this situation changes when air gap is present. In this case simultaneous solvent evaporation and moisture (non-solvent) condensation causes a local viscosity increase in the outer region of the fiber prior to immersion into coagulant bath.

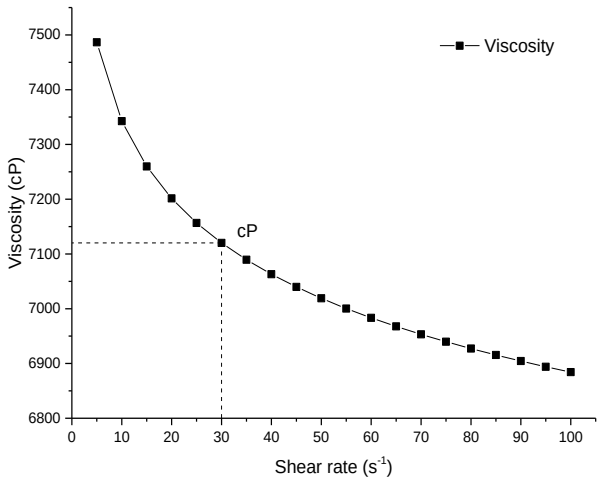

Figure 4 Viscosity of ceramic suspension containing 70.0% NiO, 22.9% NMP, 7.0% PESf and 1.0% Arlacel

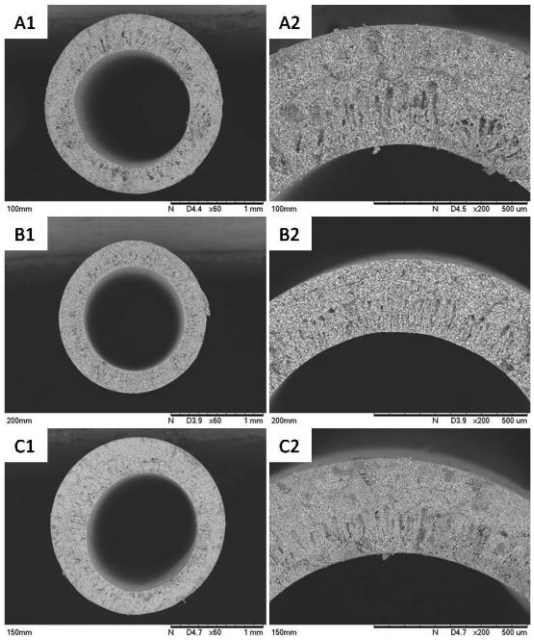

Figure 5 SEM images of cross sections membrane M1 (A), M2 (B), and M3 (C)

As air gap increase, the nascent fiber time exposed to the atmosphere also increases. The viscosity of the outer region increases while finger-like voids originating at the inner surface penetrate into the fiber cross-section. As the nascent fiber makes contact with the non-solvent bath (coagulant water bath), the increased viscosity of the outer region due to exposure to the atmosphere hampers the growth of finger-like voids at the outer edge. However, non-solvent influx from the precipitation bath does still occur for 100 mm and 150 mm air gap, which further increased the suspension viscosity as it penetrates the nascent fiber cross section. The viscosity right in front of growing finger-like voids rapidly increased and

eventually limiting its length. Higher air gap results decrease of small finger-like voids in outer region and eventually completely suppressed at air gap of 200 mm.

Detail analysis of SEM images in Figure 5 are shown in Figure 6 and Figure 8. Figure 6 shows effects of air gap length on inner and outer finger-like voids length. In general it shows decrease in both inner and outer finger-like voids length. Outer finger-like voids structure decreases from 69.965 µm (covering 19.38% of cross section length) for M1 to 39.269 µm (12.37%) for M2 and completely diminished (0%) for hollow fiber M3. In absent of finger-like voids in outer surface for hollow fiber M3, there is dense thin layer skin formed on the outer hollow fiber membrane surface. This structure agrees with morphology asymmetric hollow fiber membrane. On the other hand, decreases in inner finger-like void is not significant with its length decrease from 139.29 µm (38.58%) to 133.17 µm (41.96%) and 134.91 µm (58.81%) for membrane M1, M2 and M3 respectively. This behaviour is due to decrease in thickness of membrane itself as shown in Figure 8 which contributes to increase of viscosity around inner finger-like voids during formation resulting slightly stunted finger-like voids formation. On the other hand percentages of finger-like voids structure shows that in absence of outer finger-like voids, inner finger-like voids covered bigger cross section surface area. Percentage of surface area covered with finger-like voids does not altered much from M1 to M3 with the value varied between 54% to 58% with the rest of cross section filled with sponge-like structure.

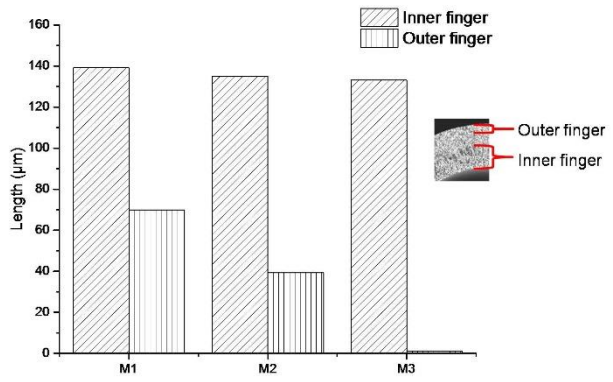

Figure 6 Inner and outer finger-like voids length for precursors hollow fiber membrane M1, M2, and M3

Figure 7 shows bending strength of M1, M2 and M3 sintered at different temperatures. The bending strength of hollow fiber, σ_F was tested using three-point bending test technique and calculated using the following equation:

$$\sigma_F = \frac{8\,F\,L\,D_1}{\pi\,(D_1^4 - D_2^4)} \quad (1)$$

Where F is the measured load at which fracture occurred (N); L is length of fiber (m) and D_1 and D_2 are outer and inner diameter respectively.

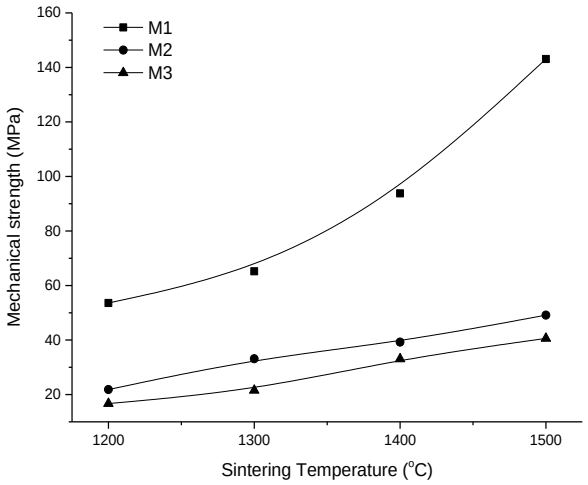

Figure 7 Mechanical strength of membrane hollow fiber M1, M2 and M3 sintered at temperature of 1200, 1300, 1400 and 1500 °C

The value of bending strength increased as sintering temperature is increased from 1200 °C to 1500 °C. Hollow fiber M1 shows the highest mechanical strength improvement, with increases from 53.60 MPa to 143.08 MPa after sintered at temperature of 1200 °C to 1500 °C (89.48 MPa increment) followed by M2 which increased from 21.85 MPa to 49.11 MPa (27.27 MPa increment) while M3 has the lowest mechanical strength improvement with increase from 16.69 MPa to 40.59 MPa (23.90 MPa increment). This increased in mechanical strength is due to increase in grain size during sintered. During sintering process, there are three stages of sintering with different purpose. As shown in Figure 3, at first stage (300 °C for 1 hour), is to dry the hollow fiber membrane, while in second stage (700 °C for 2 hours) is to burn off any remaining organic material such as PESf that has served its purpose as organic binder. During the final stage (at target temperature for 3 hours), both densifying and non-densifying mechanisms competes with each other. However, in this case the densifying mechanism out weight the non-densification mechanism, which results in densification instead of coarsening of membrane. This densification increase as sintering temperature is increased, producing higher mechanical strength of membrane.

Comparison between M1, M2 and M3 shows that M1 gives highest mechanical strength followed by M2 and M3. This is due to physical structure of membrane itself as shown in Figure 8. M1 has the thickest of membrane with thickness of 0.361 mm compare to M2, 0.317 mm and M3, 0.2294 mm. Membrane that is thicker give advantages in mechanical strength. On the other hand, Figure 8

shows that as air gap increases, internal diameter, Di slightly decreases (by 12.01%) from 1.257 mm, 1.226 mm and 1.106 mm for M1, M2 and M3 respectively. This decrease becomes more significant (by 20.58%) for outer diameter, Do which decreases from 1.9308 mm, 1.226 mm and 1.106 mm for M1, M2 and M3 respectively.

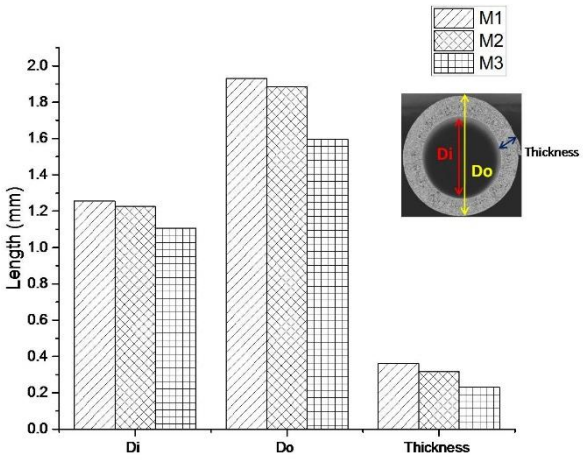

Figure 8 Inner diameter (Di), Outer diameter (Do) and membrane thickness of M1, M2 and M3

As air gap is increases, the elongation effects induced by gravitational force increases as describe in Figure 9. These results in smaller outer radius of membrane hollow fiber compare to hollow fiber membrane spun at smaller air gap distance.

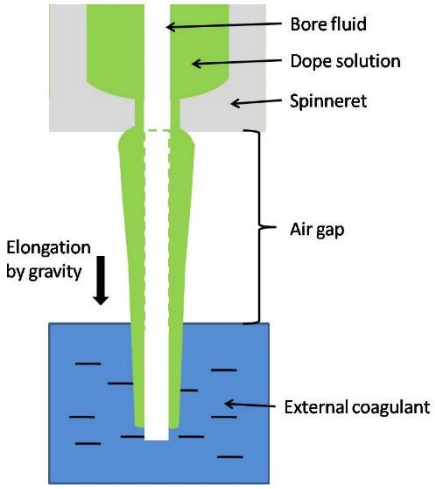

Figure 9 Coagulation in hollow fiber spinning

4.0 CONCLUSIONS

Hollow fibers prepared from NiO/NMP/PESf/Alracel spinning suspension below the threshold critical suspension viscosity produces finger-like voids originate from both inner and outer surface due to unstable viscous fingering that occurs at the interface between suspension and the non-solvent. An increase in air gap length increased the time of hollow fiber outer surface exposure to atmosphere before in contact with non-solvent subsequently diminished the formation of finger-like voids. The air-gap and suspension viscosity are both important in determining the formation of finger-like voids from inner and outer surface membrane. The abilities to control the morphology of hollow fiber membrane give advantages on how to optimize the usage of hollow fiber membrane. Asymmetric structure with long finger-like voids, and thin separation layer is favorable due to high permeation. This membrane can work as support to graphene growth as well as separation membrane itself for various purpose such as desalination, oily wastewater treatment and heavy metal removal.

Acknowledgement

The authors gratefully acknowledge the financial support from the Ministry of Education Malaysia under the Higher Institution Centre of Excellence Scheme (Project Number: R.J090301.7846.4J201) and Universiti Teknologi Malaysia under Research University Grant Tier 1 (Project Number: Q.J130000.2546.12H25). The authors would also like to thank Research Management Centre, Universiti Teknologi Malaysia for the technical support.

References

[1] Shirazi, S., Lin, C. J., & Chen, D. 2010. Inorganic Fouling Of Pressure-Driven Membrane Processes-A Critical Review. *Desalination*. 250(1): 236-248.
[2] Kanawka, K., Othman, M. H. D., Wu, Z., Droushiotis, N., Kelsall, G., & Li, K. 2011. A Dual Layer Ni/Ni-YSZ Hollow Fibre For Micro-Tubular SOFC Anode Support With A Current Collector. *Electrochemistry Communications*. 13(1): 93-95.
[3] Jamil, S. M., Othman, M. H. D., Rahman, M. A., Jaafar, J., Ismail, A. F., Li, K. 2015. Recent Fabrication Techniques For Micro-Tubular Solid Oxide Fuel Cell Support: A Review. *Journal of the European Ceramic Society*. 35(1): 1-22.
[4] Droushiotis, N., Torabi, A., Othman, M. H. D., Etsell, T. H., Kelsall, G. H. 2012. Effects Of Lanthanum Strontium Cobalt Ferrite (LSCF) Cathode Properties On Hollow Fibre Micro-Tubular SOFC Performances. *Journal of Applied Electrochemistry*. 42(7): 517-526.
[5] Bhave, R. 2012. *Inorganic Membranes Synthesis, Characteristics And Applications: Synthesis, Characteristics, And Applications*. Springer Science & Business Media.
[6] Biesheuvel, P. M., & Verweij, H. 1999. Design Of Ceramic Membrane Supports: Permeability, Tensile Strength And Stress. *Journal of Membrane Science*. 156(1): 141-152.
[7] Kingsbury, B. F., & Li, K. 2009. A Morphological Study Of Ceramic Hollow Fiber Membranes. *Journal of Membrane Science*. 328(1): 134-140.
[8] Kim, J. H., & Lee, K. H. 1998. Effect Of PEG Additive On Membrane Formation By Phase Inversion. *Journal of Membrane Science*. 138(2): 153-163.

[9] Wienk, I. M., Boom, R. M., Beerlage, M. A. M., Bulte, A. M. W., Smolders, C. A., & Strathmann, H. 1996. Recent Advances In The Formation Of Phase Inversion Membranes Made From Amorphous Or Semi-Crystalline Polymers. *Journal of Membrane Science*. 113(2): 361-371.
[10] Smolders, C. A., Reuvers, A. J., Boom, R. M., & Wienk, I. M. 1992. Microstructures In Phase-Inversion Membranes. Part 1. Formation Of Macrovoids. *Journal of Membrane Science*. 73(2-3): 259-275.
[11] Boom, R. M., Wienk, I. M., Van den Boomgaard, T., & Smolders, C. A. 1992. Microstructures In Phase Inversion Membranes. Part 2. The Role Of A Polymeric Additive. *Journal of Membrane Science*. 73(2): 277-292.
[12] Tan, X., Liu, Y., & Li, K. 2005. Preparation Of LSCF Ceramic Hollow-Fiber Membranes For Oxygen Production By A Phase-Inversion/Sintering Technique. *Industrial & Engineering Chemistry Research*. 44(1): 61-66.
[13] Liu, S., Li, K., & Hughes, R. 2003. Preparation Of Porous Aluminium Oxide (Al_2O_3) Hollow Fibre Membranes By A Combined Phase-Inversion And Sintering Method. *Ceramics International*. *29*(8): 875-881.
[14] Tan, X., Liu, Y., & Li, K. 2005. Preparation Of LSCF Ceramic Hollow-Fiber Membranes For Oxygen Production By A Phase-Inversion/Sintering Technique. *Industrial & Engineering Chemistry Research*. 44(1): 61-66.
[15] Tan, X., Liu, S., & Li, K. 2001. Preparation And Characterization Of Inorganic Hollow Fiber Membranes. *Journal of Membrane Science*. 188(1): 87-95.